

Analysis of torsional barrier height of HSNO as the simplest S-nitrosothiol

REZA FAZAEI^{a,*}, MOHAMMAD SOLIMANNEJAD^b and ABDOLVAHAB SEIF^b

^aModeling and Optimization Research Center in Science and Engineering, South Tehran Branch, Islamic Azad University, Tehran, Iran, P.O. Box 11365–4435

^bQuantum Chemistry Group, Department of Chemistry, Faculty of Sciences, Arak University, Arak 38156-8-8349, Iran
e-mail: r_fazaeli@azad.ac.ir

MS received 10 September 2012; revised 5 December 2012; accepted 21 January 2013

Abstract. Torsional barrier height of thionitrous acid is analysed with Gaussian-2(G2), quadratic complete basis set (CBS-Q) and DFT-B3LYP/CBS-Q (CBS-QB3) methods. In agreement with purely intuitive arguments, it was determined that the *cis* to *trans* barrier height is nearly 5.7–6.3 kcal mol⁻¹. In addition, the stability of rotation as function of competing dissociation pathways and also result of natural bond orbital analysis are discussed.

Keywords. Gaussian-2 (G2); CBS-Q; CBS-QB3; torsional barrier; thionitrous acid (HSNO).

1. Introduction

S-nitrosothiol consists of molecules of biological and medicinal interest, which cause vasodilation of veins and arteries and inhibition of platelet aggregation, through the release of nitric oxide (NO).^{1,2} The weakness of S–NO bonds in S-nitrosothiol is clearly evident from their high reactivity.^{1,2} Thionitrous acid (HSNO) can be considered as the simplest S-nitrosothiol. There are many reasons behind the significant interest in compounds which include sulphur-containing groups.^{3–6} Recently, *ab initio* studies on the electronic structures and relative energies of HSNO isomers have been reported.^{7,8} To the best of our knowledge, no comparative computational studies about torsional potential of thionitrous acid have been carried out. In this study, we perform a series of *ab initio* calculations in order to compute the torsional barrier height of HSNO and also discuss the stability of rotation as a function of three competing dissociation pathways. Natural bond orbital (NBO) analysis is also carried out to obtain deeper insight into the reason behind the order of stability for various conformers.

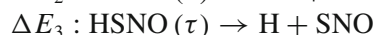
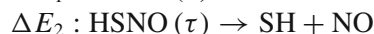
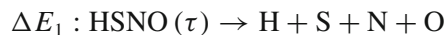
2. Computational methods

All Gaussian-2 (G2), quadratic complete basis set (CBS-Q) and DFT-B3LYP/CBS-Q (CBS-QB3), calculations were performed with the GAUSSIAN 98⁹ set of

codes. More information about the employed methodology is available in literature.¹⁰ However, essentially the CBS-Q method uses the B3LYP/CBSB7 method to perform geometrical optimizations and frequency computation, while the G2 and CBS-Q methods use MP2 geometries and Hartree-Fock (HF) frequencies, with 6-311G(d), and 6-31G(d') basis sets, respectively.

3. Results and discussion

HSNO is planar molecule—its *cis* and *trans* forms are shown in figure 1. In table 1, other species used in our analysis of the decomposition of the HSNO rotation along τ are shown. Table 2 shows the computed relative total energies (expressed in kcal mol⁻¹) for varying HSNO dihedral angle τ in degrees (°). The barrier for conversion of *cis* to *trans* conformer is estimated as the energy difference between the *cis* form and the transition state. In this particular case, the transition state was found to occur at 87 degrees as depicted in figures 1 and 2. In agreement with purely intuitive arguments, it was determined that the *cis* to *trans* barrier height is nearly 5.7–6.3 kcal mol⁻¹. We next investigated the stability (relative to dissociation) for various regions of HSNO (shown in table 3) for the processes of atomization (1), S–N bond cleavage (2), and hydrogen abstraction (3) that may occur in the atmosphere.



*For correspondence

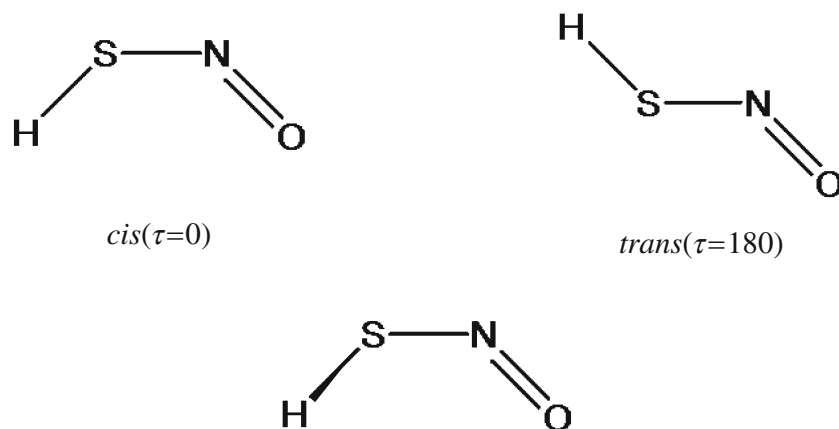


Figure 1. *Cis* and *trans* conformers of thionitrous acid (HSNO) and transition state for conversion of *cis* to *trans* conformer. TS ($\tau = 86.9, 86.3,$ and 87.7 degrees at G2, CBS-Q, and CBS-QB3, respectively).

Table 3 shows the relative energies (ΔE) for different pathways. It can be seen in table 3 (it should be rather obvious) that *trans* decomposition energies are higher than all other pathways. The ΔE_1 : HSNO (τ) \rightarrow H+S+N+O, pathways passes the highest energies of reaction, thus emphasizing the stability of this species towards atomization (in atmosphere or veins, for example), and lowest energy pathway is ΔE_2 : HSNO (τ) \rightarrow SH+NO that gives radical species as products. From our energy analysis, a homolytic cleavage of bond S–N mechanism should be the most likely dissociation pathway.

In order to obtain a deeper insight into the reasons behind the order of stability for various conformers in the present study system, as well as to obtain more information about the direction and magnitude of intramolecular charge-transfer (CT) interaction, NBO^{11–16} analysis was performed for all points on the relaxed torsional potential energy surface (PES). A second-order perturbation theory (SOPT) analysis of the Kohn–Sham one-electron analogue of the Fock matrix within the NBO basis was carried out for selected geometries obtained with partial geometry optimization for a fixed torsional angle.

Table 1. Computed total energies (in Hartrees) for species in decomposition of HSNO.

Species	G2	CBS-Q	CBS-QB3
H	−0.498584	−0.498402	−0.498402
S	−397.653524	−397.655471	−397.655956
N	−54.516543	−54.518827	−54.519121
O	−74.980614	−74.985643	−74.986213
SH	−398.284611	−398.287447	−398.288300
NO	−129.737606	−129.744709	−129.746108
SNO	−527.434934	−527.464615	−527.453917

Within the NBO approach, the estimated energetic effects due to CT interactions are given by the SOFT expressions from ref. 11:

$$\Delta E^{(2)}\psi_{\text{don}} \rightarrow \psi_{\text{acc}} \approx 2 \left(\frac{\langle \psi * | \hat{F} | \psi \rangle}{\varepsilon_{\text{acc}} - \varepsilon_{\text{don}}} \right)^2, \quad (1)$$

where ε_i is a diagonal NBO matrix element of the Fock operator F . The result from the SOPT analyses for all the considered structures are summarized in table 4. Only the most relevant CT contributions (in an energetic sense) and their variations with the change in torsional angle τ are listed. It can be seen in table 4, that the CT from the LP(O) orbital to the S–N antibonding orbital (LP(O) \rightarrow BD*S–N) state, is energetically the most significant contribution to the overall system stability when CT interaction is in question. It also shows most pronounced torsional angle dependence, the corresponding $\Delta E^{(2)}$ value increasing from 0 to 90°, and significantly decreasing as the angle τ increases

Table 2. Computed relative total energies (in kilocalories per mole) for varying HSNO dihedral angle (τ) in degrees (°).

τ (°)	G2	CBS-Q	CBS-QB3
0	1.030	1.003	0.981
20	1.986	2.090	2.011
40	3.902	4.124	4.441
60	6.495	6.811	6.265
80	8.000	8.324	7.620
100	7.785	8.133	7.413
120	5.838	6.180	5.622
140	3.515	3.749	3.506
160	1.005	1.046	1.015
180	0	0	0

Table 3. Relative energy (ΔE) of the dissociation energy pathways (kcal mol⁻¹) for ΔE_1 : HSNO (τ) \rightarrow H+S+N+O, ΔE_2 : HSNO (τ) \rightarrow HS+NO and ΔE_3 : HSNO (τ) \rightarrow H+SNO.

τ (°)	G2	CBS-Q	CBS-QB3
ΔE_1			
0	262.863	263.750	263.302
20	261.801	262.663	262.272
40	259.991	260.629	259.843
60	257.398	257.942	258.019
80	255.893	256.430	256.662
100	256.109	256.620	256.870
120	258.056	258.573	258.662
140	260.385	261.004	260.778
160	262.889	263.707	263.269
180	263.893	264.753	264.283
ΔE_2			
0	28.836	29.182	28.168
20	27.773	28.096	27.138
40	25.963	26.061	24.708
60	23.370	23.374	22.885
80	21.865	21.861	21.528
100	22.081	22.052	21.736
120	24.028	24.006	23.527
140	26.351	26.436	25.643
160	28.861	29.139	28.133
180	29.865	30.185	29.149
ΔE_3			
0	84.495	72.567	79.679
20	83.432	71.480	78.649
40	81.622	69.446	76.219
60	79.029	66.759	74.396
80	77.523	65.246	73.039
100	77.740	65.437	73.247
120	79.687	67.390	75.038
140	82.010	69.821	77.154
160	84.520	72.524	79.645
180	85.524	73.570	80.660

to 180° for the most intramolecular CT contribution as shown in figure 3(a). Other significant contributions to the overall intramolecular CT are LP(S) \rightarrow BD*N-O, BD S-H \rightarrow BD*S-N, BD S-H \rightarrow BD*N-O, and BD S-N \rightarrow BD*NO.

Finally, the energy barriers calculated using the distinct theoretical approaches mentioned above were fitted to a potential function, represented by nine term truncated Fourier series,¹⁷ as described in (2).

$$V(\tau) = \sum_{i=1}^9 (V_i/2) (1 - \cos(i\tau)), \quad (2)$$

where τ is the torsional angle which is allowed to vary from 0 to 180° in steps of 20 degrees. It should be mentioned that in (2), $V(\tau)$ is the relative energy at the rotational angle τ , which has to be defined as (180° - τ) since *trans* was selected as the energy origin. The

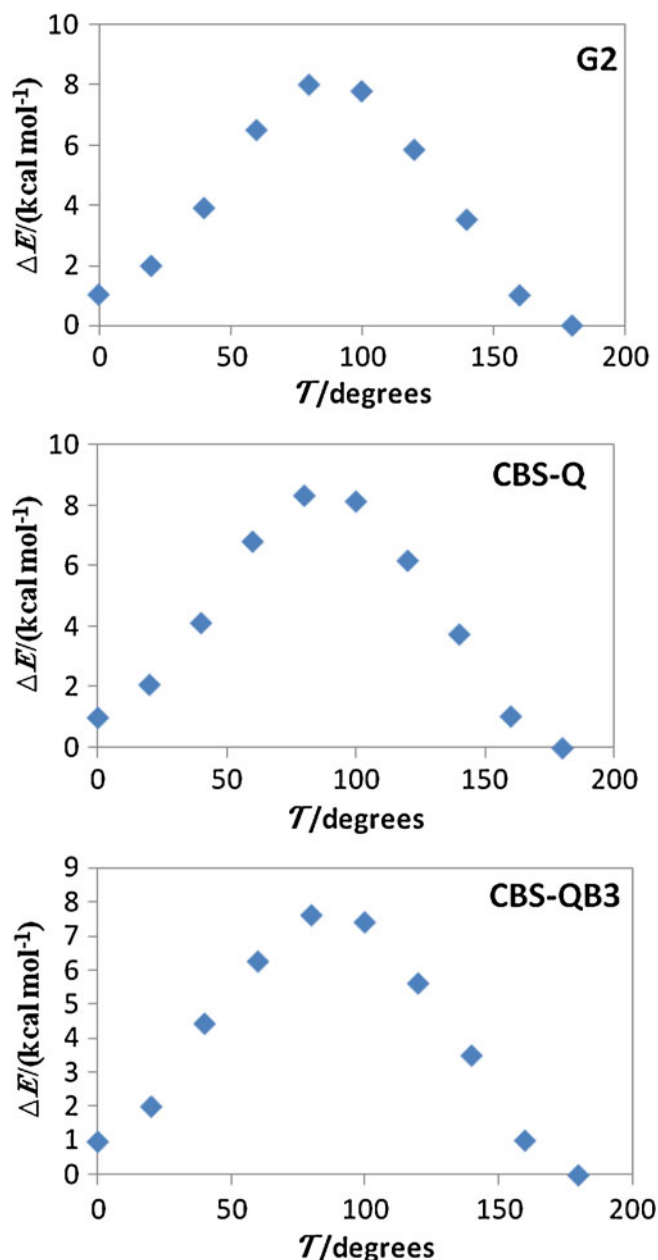


Figure 2. Relative energies of HSNO molecule versus torsional angle at three computational levels.

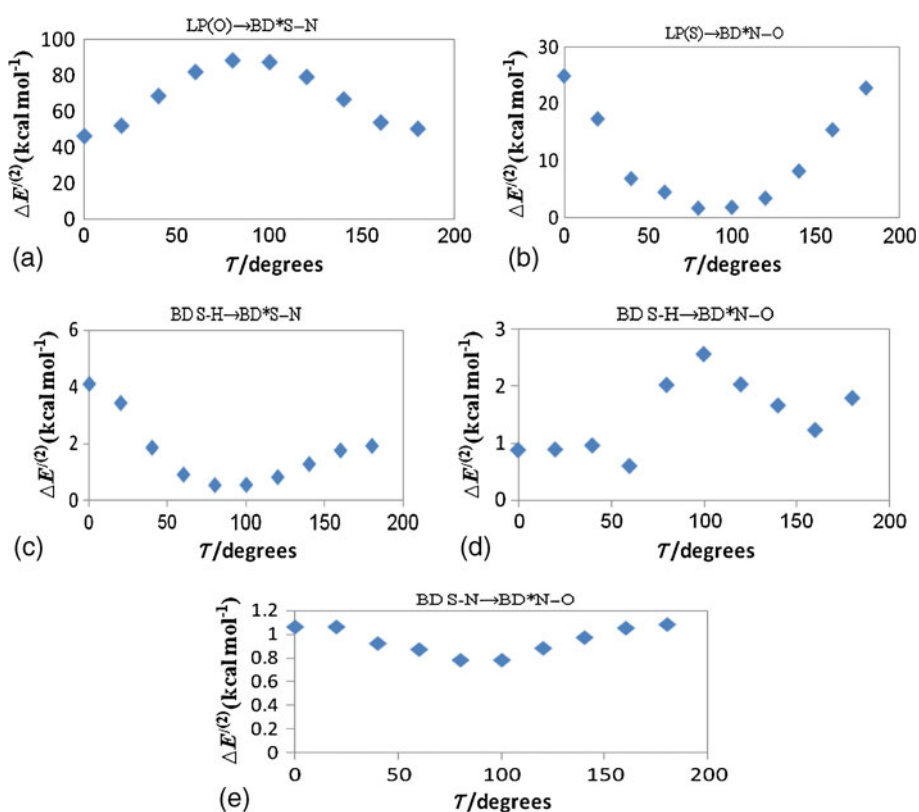
potential parameters obtained from the fitting are shown in table 5.

4. Conclusions

In this study, we have presented the results of our G2, CBS-Q and CBS-QB3 calculations on the torsional dissociation and rotation barrier of HSNO. Our methods are generally in good agreement with one another regardless of the choice of optimization method for the first steps of the Gaussian calculations. It is interesting to note that the HSNO torsional potential correlated

Table 4. Result of the second-order perturbation theory (SOPT) analysis of the Kohn–Sham one analogue of the Fock matrix within the NBO basis for selected geometries obtained with partial geometry optimization for a fixed torsional angle.

		$\tau(^{\circ})$										
Donor	Acceptor	0	20	40	60	80	100	120	140	160	180	
LP(O)	BD*S–N	46.43	52.18	68.67	82.02	88.38	87.37	79.23	66.81	53.98	50.46	
LP(S)	BD*N–O	25.00	17.42	6.87	4.48	1.63	1.81	3.41	8.19	15.49	22.88	
BD S–H	BD*S–N	4.10	3.43	1.86	0.91	0.54	0.55	0.82	1.28	1.76	1.92	
BD S–H	BD*N–O	0.88	0.89	0.96	0.60	2.02	2.56	2.03	1.66	1.23	1.79	
BD SN	BD*NO	1.06	1.06	0.92	0.87	0.78	0.78	0.88	0.97	1.05	1.08	

**Figure 3.** Variation of energy of charge transfer energies with the torsional angle: (a) (LP(O)→BD*S–N), (b) (LP(S)→BD*N–O), (c) (BD S–H→BD*S–N), (d) (BD S–H→BD*N–O), and (e) (BD S–N→BD*NO).**Table 5.** Result of a fit of the data in table 3 (relative energy) to the Fourier series as $V(\tau) = \sum_{i=1}^9 (V_i/2) (1 - \cos(i\tau))$.

	v_1	v_2	v_3	v_4	v_5	v_6	v_7	v_8	v_9
G2	0.932	7.513	0.021	0.004	0.210	0.110	−0.019	0.017	−0.115
CBS-Q	0.941	7.861	0.048	0.107	0.190	0.106	−0.043	0.023	−0.135
CVS-QB3	1.111	7.058	−0.100	0.390	−0.035	0.278	0.007	−0.178	−0.001

very well with a potential function, represented by nine terms truncated Fourier series.

References

1. Wang K, Zhang W, Xian M, Hou Y C, Chen X C, Cheng J P and Wang P G 2000 *Curr. Med. Chem.* **7** 821
2. Williams D L H 1999 *Acc. Chem. Res.* **32** 869
3. Sumathi R, Peyerimhoff S D and Sengupta D 1999 *J. Phys. Chem.* **A1031** 772
4. Smith D, Adams N G, Giles K and Herbst E 1988 *Astron. Astrophys.* **200** 191
5. Millar T J and Herbst E 1990 *Astron. Astrophys.* **231** 466
6. Anicich G 1993 *J. Phys. Chem. Ref. Data* **22** 1469
7. Timerghazin Q K, English A M and Peslherbe G H 2008 *Chem. Phys. Lett.* **454** 24
8. Timerghazin Q K, Peslherbe G H and English A M 2008 *Phys. Chem. Chem. Phys.* **10** 1532
9. Frisch M J, Trucks G W, Schlegel H B, Scuseria G E, Robb M A, Cheeseman J R, Zakrzewski V G, Montgomery J A, Stratmann R E, Burant J C, Dapprich S, Millam J M, Daniels A D, Kudin K N, Strain M C, Farkas O, Tomasi J, Barone V, Cossi M, Cammi R, Mennucci B, Pomelli C, Adamo C, Clifford S, Ochterski J, Petersson G A, Ayala P Y, Cui Q, Morokuma K, Malick D K, Rabuck A D, Raghavachari K, Foresman J B, Cioslowski J, Ortiz J V, Stefanov B B, Liu G, Liashenko A, Piskorz P, Komaromi I, Gomperts R, Martin R L, Fox D J, Keith T, Al-Laham M A, Peng C Y, Nanayakkara A, Gonzalez C, Challacombe M, Gill P M W, Johnson B G, Chen W, Wong M W, Andres J L, Head-Gordon M, Replogle E S and Pople J A 1998 GAUSSIAN 98 (Revision A.6). Gaussian Inc., Pittsburgh
10. Foresman G B and Frisch A E 1996 *Exploring chemistry with electronic structure methods* (2nd edn). Gaussian, Inc., Pittsburgh, PA
11. Curtiss L, Pochatko D G, Reed A E and Weinhold F 1985 *J. Chem. Phys.* **82** 2679
12. Reed A E and Weinhold F 1985 *J. Chem. Phys.* **83** 1736
13. Foster J P and Weinhold F 1980 *J. Am. Chem. Soc.* **102** 7211
14. Reed A E and Weinhold F 1983 *J. Chem. Phys.* **78** 4066
15. Reed A E, Weinhold F, Curtiss L A and Pochatko D G 1986 *J. Chem. Phys.* **84** 5687
16. Reed A E, Weinstock R B and Weinhold F 1985 *J. Chem. Phys.* **83** 735
17. Meerts W L and Osier I 1982 *J. Mol. Spectrosc.* **94** 38